Journal of Solid State Chemistry **166,** 382–388 (2002)
doi:10.1006/jssc.2002.9609

# Electrical Resistivity, Magnetic Susceptibility, X-Ray Photoelectron Spectroscopy, and Electronic Band Structure Studies of $Cu_{2.33-x}V_4O_{11}$

P. Rozier,*[,1] J. Galy,* G. Chelkowska,† H.-J. Koo,‡ and M.-H. Whangbo‡

*CEMES/CNRS, 29 rue Jeanne Marvig, BP4347, 31055 Toulouse Cedex 4, France; †Institute of Physics, University of Silesia, Uniwersytecka 4, 40-007 Katowice, Poland; and ‡Department of Chemistry, North Carolina State University, Raleigh, North Carolina 27695-8204

Received February 7, 2002; in revised form March 27, 2002; accepted April 5, 2002

**The electronic and physical properties of $Cu_{2.33}V_4O_{11}$ were characterized by electrical resistivity, magnetic susceptibility and X-ray photoelectron spectroscopy (XPS) measurements and by tight-binding electronic band structure calculations. Attempts to prepare $Cu_{2.33-x}V_4O_{11}$ outside its narrow homogeneity range led to a mixture of $Cu_{2.33}V_4O_{11}$, $CuVO_3$ and $\beta$-$Cu_xV_2O_5$. The magnetic susceptibility data show no evidence for a magnetic/structural transition around 300 K. The XPS spectra of $Cu_{2.33}V_4O_{11}$ reveal the presence of mixed valence in both Cu and V. The $[Cu^+]/[Cu^{2+}]$ ratio is estimated to be 1.11 from the Cu $2p_{3/2}$ peak areas, so $[V^{4+}]/[V^{5+}] = 0.56$ by the charge balance. Our electronic structure calculations suggest that the oxidation state of the Cu ions is +2 in the channels of $CuO_4$ tetrahedra, and +1 in the channels of linear $CuO_2$ and trigonal planar $CuO_3$ units. This predicts that $[Cu^+]/[Cu^{2+}] = 1.33$ and $[V^{4+}]/[V^{5+}] = 0.50$, in good agreement with those deduced from the XPS study.** 

## 1. INTRODUCTION

Ternary vanadium oxide bronzes of approximate formula $M_xV_2O_5$ exhibit a wide variety of crystal structures (1) and chemical/physical properties, which are governed by the nature and non-stoichiometry of the element $M$ (e.g., alkali, alkaline earth, Cu, Ag, Zn) and by the associated mixed-valence in vanadium. Among these oxides, the copper–vanadium–bronze family ($M$ = Cu) is of special interest because both Cu and V can exhibit mixed-valence ($Cu^+/Cu^{2+}$ and $V^{4+}/V^{5+}$) (2–5). In 1971, Galy *et al.* (6) isolated a new phase that was formulated as $Cu_xV_4O_{11}$ ($Cm$, $a = 15.38$ Å, $b = 3.61$ Å, $c = 7.37$ Å, $\beta \approx 102^\circ$). On the basis of examining this phase for a wide range of composition, Saito *et al.* (7) reported that $Cu_xV_4O_{11}$ undergoes a magnetic/structural transition at $T_c \approx 300$ K, and this transition in samples with $x > 2$ involves a charge transfer between the Cu and V ions. More recently, Kato *et al.* (8) determined an incommensurately modulated structure of $Cu_xV_4O_{11}$ ($x = 2.12$), which suggested that in the two types of Cu ion channels (running along the $b$-direction) present between adjacent $V_4O_{11}$ layers, the Cu ion distribution is random in one type channels but modulated in the other type channels.

The structural chemistry of $Cu_xV_4O_{11}$ was clarified by several investigations (9–11). The existence of an incommensurate modulation in this phase was confirmed by the Bragg and Weissenberg diagrams (9). On the basis of the average structure of $Cu_xV_4O_{11}$ determined from single crystal X-ray diffraction (XRD) measurements, this phase was reformulated as $Cu_{2.33-x}V_4O_{11}$ ($x \geq 0$) to emphasize the maximum possible value of the Cu ion occupancy (i.e., 2.33) (9). The average structure consists of four non-equivalent Cu and four non-equivalent V atom positions (Fig. 1). Temperature-dependent electron diffraction measurements of $Cu_{2.33-x}V_4O_{11}$ show two distinct incommensurate modulations that involve three-dimensional ordering of Cu ions in the two types of Cu ion channels (10); $q_1 = 0.5c^* + \sim 0.12b^*$ and $q_2 = \pm 0.5a^* + \sim 0.16b^*$, with the latter occurring at low temperatures. The refinement of our incommensurate structure, carried out at both room and low temperatures by single-crystal XRD (11), shows that the modulations are directly related to Cu ion ordering in both types of Cu ion channels.

To verify the magnetic/structural transition at 300 K reported by Saito *et al.* (7), it is necessary to study the physical properties of homogeneous samples. In the present work, we prepare homogeneous samples of $Cu_{2.33}V_4O_{11}$ and characterize their electronic and physical properties by electrical resisitivity, magnetic susceptibility and X-ray photoelectron spectroscopy (XPS) measurements. Results of these experiments are then analyzed by electronic band structure calculations using the extended Hückel tight-

[1] To whom correspondence should be addressed. Fax: +33-5-62-25-79-99. E-mail: rozier@cemes.fr.



0022-4596/02 $35.00

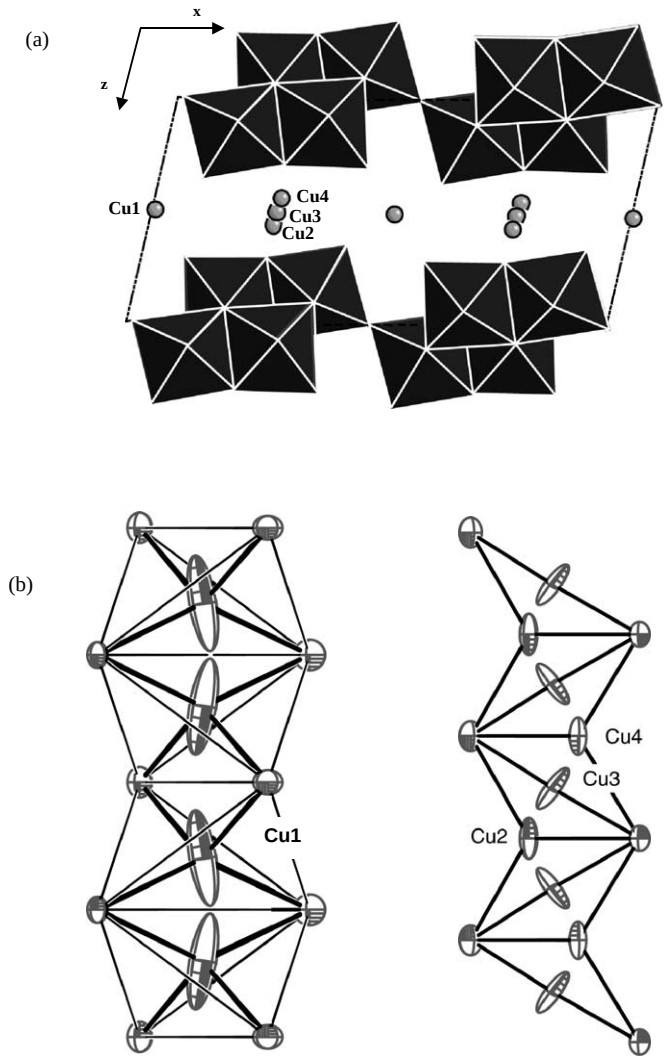


**FIG. 1.** (a) Schematic projection view of the crystal structure of $Cu_{2.33}V_4O_{11}$ along the *b*-direction, where the $VO_6$ octahedra are presented in polyhedral view. (b) Schematic views of the two channels of Cu atoms. The channel of Cu(1) atoms is made up of edge-sharing $Cu(1)O_4$ tetrahedra, and the channel of Cu(2), Cu(3) and Cu(4) atoms consists of the $Cu(2)O_3$ and $Cu(4)O_3$ trigonal planar and the $Cu(3)O_2$ linear units.

**TABLE 1**

**Exponents $\zeta_i$ and Valence Shell Ionization Potentials $H_{ii}$ of Slater-Type Orbitals $\chi_i$ Used for Extended Hückel Tight-Binding Calculation[a]**

| Atom | $\chi_i$ | $H_{ii}$ (eV) | $\zeta_i$ | $c_1$[b] | $\zeta_i'$ | $c_2$[b] |
|---|---|---|---|---|---|---|
| V | 4*s* | −8.81 | 1.697 | 1.0 | | |
| V | 4*p* | −5.52 | 1.260 | 1.0 | | |
| V | 3*d* | −11.0 | 5.052 | 0.3738 | 2.173 | 0.7546 |
| O | 2*s* | −32.3 | 2.688 | 0.7076 | 1.675 | 0.3745 |
| O | 2*p* | −14.8 | 3.694 | 0.3322 | 1.659 | 0.7448 |

[a] $H_{ii}$'s are the diagonal matrix elements $\langle \chi_i | H^{\text{eff}} | \chi_i \rangle$, where $H^{\text{eff}}$ is the effective Hamiltonian. In our calculations of the off-diagonal matrix elements $H^{\text{eff}} = \langle \chi_i | H^{\text{eff}} | \chi_j \rangle$, the weighted formula was used (see Ref. (16)).

[b] Contraction coefficients used in the double-zeta Slater-type orbital.

binding method (12,13). The atomic parameters used for our calculations are listed in Table 1.

## 2. EXPERIMENTAL

### 2.1. Synthesis

CuO, $V_2O_5$ (Aldrich 99.99%) and $V_2O_4$ were used as starting materials. $V_2O_4$ was obtained by heating a stoichiometric mixture of $V_2O_3$ and $V_2O_5$ under vacuum for 12 h. $V_2O_3$ was obtained by a treatment of $V_2O_5$ under hydrogen flux. The mixture of stoichiometric amounts of starting oxides, after grinding, was sealed in a quartz ampoule under vacuum and heated up to 600°C for 12 h. Well-crystallized samples were obtained by re-heating under the same conditions. The quality of products was checked by X-ray powder diffraction (XRPD). It should be emphasized that $Cu_{2.33}V_4O_{11}$ represents the maximum Cu content expected from a more general formula $Cu_{2.33-x}V_4O_{11}$. Our attempts to prepare samples of $Cu_{2.33-x}V_4O_{11}$ with $x$ varying in a wide range show that the homogeneity domain is very narrow. For instance, synthesis carried out with an expected $x$ as low as 0.1 leads to a mixture of $Cu_{2.33}V_4O_{11}$, $CuVO_3$ and $\beta$-$Cu_xV_2O_5$.

Upon heating above the melting point, $Cu_{2.33}V_4O_{11}$ compound is quickly decomposed in several other vanadium oxide bronzes. This prevented us from growing single crystals suitable for electrical measurements. Thus, powder samples were pressed under 1 T to form pellets used for XPS and electric conductivity measurements. The sintering was achieved by heat treatment under vacuum at 620°C for 12 h.

### 2.2. Crystallographic Study

XRPD data were obtained using a Seifert XRD 3000 TT diffractometer with monochromatized Cu$K\alpha$ radiation ($\lambda = 1.5418$ Å). X-ray profiles were measured in the $\theta$ range $2 \leq \theta \leq 40^\circ$ in a step scan mode with a counting time of 10 s and an angular step of 0.01° in $\theta$.

### 2.3. Electrical Resistivity

Platinum wires were glued to a sintered pellet using platinum conducting paint, and the electrical resistivity was measured on the basis of the four-probe direct current method using a Keithley (224 and 181) coupled apparatus in the temperature range $80 < T < 850$ K. To prevent the transition metals V and Cu from oxidation, all the

measurements were carried out under helium. Measurement cycles were repeated at least two times to confirm the reproducibility of results.

### 2.4. Magnetic Susceptibility

Magnetic susceptibility was measured between the liquid helium temperature and 500 K using a SQUID magnetometer MPMS-5 Quantum Design in a sweep two temperature mode (1 K/min, acquisition every 2 K). The operating magnetic field strength was 1 kG. Diamagnetic corrections were made.

### 2.5. XPS

An ESCA spectrometer Physical Electronics (PHI 5700/660) with monochromatic Al$K\alpha$ radiation ($h\nu = 1486.6$ eV) was used for our XPS study. The spectra of a sintered sample were measured after breaking it in a high vacuum ($10^{-9}$ Torr). All spectra were recorded at room temperature and were calibrated using a gold foil, which has the binding energy of the Au $4f_{3/2}$ level at 84.0 eV. The energy resolution was 0.3 eV.

## 3. ELECTRICAL RESISTIVITY

The electrical resistivity $\rho$ of $Cu_{2.33}V_4O_{11}$ between 120 and 300 K is shown in Fig. 2a, and that between 270 and 820 K in Fig. 2b. The compound is weakly metallic above $\sim$600 K, and exhibits a semiconductor-like behavior below $\sim$600 K. The temperature dependence of the conductivity $\sigma$ in a non-metallic state can be modeled by the expression, $\sigma = A\exp(-E_a/RT)$, where $E_a$ is the activation energy. The Arrhenius plot, $\ln\sigma$ vs $1/T$, shown in Fig. 3a reveals that in the region between $\sim$100 K and room temperature, the pre-exponential factor $A$ is proportional to $T^2$, and $E_a$ is very small (i.e., 0.03 eV). The Arrhenius plot presented in Fig. 3b shows that the resistivity above 300 K has a complex behavior. The lower-temperature behavior is maintained up to 370 K. In the 370–530 K region, $E_a$ increases slightly (to 0.04 eV) but the pre-exponential factor does not depend on temperature. In the 530–620 K region, $E_a$ increases to 0.2 eV, a value typically expected for the electron hoping process associated with $V^{4+}$ and $V^{5+}$ sites (14). Above 620 K the temperature dependence of the resistivity is characteristic of a metal.

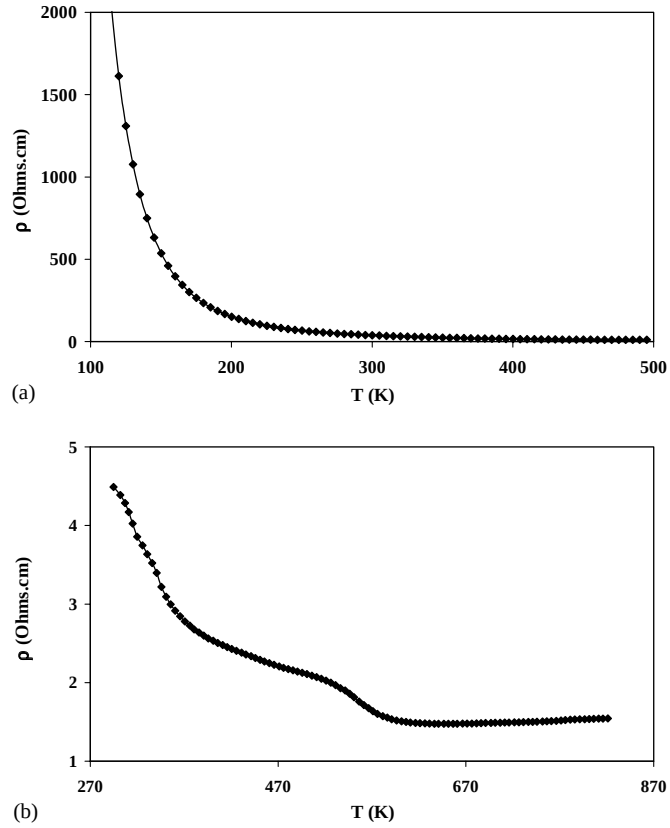


**FIG. 2.** Temperature dependence of the electrical resistivity of $Cu_{2.33}V_4O_{11}$ in the (a) low- and (b) high-temperature regions.

## 4. MAGNETIC SUSCEPTIBILITY

The temperature dependence of the magnetic susceptibility of $Cu_{2.33}V_4O_{11}$ is presented in Fig. 4a. Between $\sim$100 K and room temperature, the susceptibility is nearly independent of temperature, which corresponds to a Pauli paramagnetic behavior expected for a metal. This is probably related to the fact that although $Cu_{2.33}V_4O_{11}$ is not metallic in the temperature region between $\sim$100 K and room temperature, the activation energy of its electrical conductivity is very small. Figure 4 shows no evidence for a magnetic transition around 300 K, contrary to the report by Saito *et al.* (7). As already pointed out, the homogeneous range of $Cu_{2.33-x}V_4O_{11}$ is very narrow, and synthesis outside this range leads to a mixture of $Cu_{2.33}V_4O_{11}$, $CuVO_3$ and $\beta$-$Cu_xV_2O_5$. The magnetic susceptibilities of $CuVO_3$ and $\beta$-$Cu_xV_2O_5$ between 80 and 300 K are presented in Fig. 4. $CuVO_3$ shows a paramagnetism while $\beta$-$Cu_xV_2O_5$ is slightly antiferromagnetic. The magnetic susceptibility curve of $Cu_{2.33-x}V_4O_{11}$ for which the copper content deviates considerably from 2.33 is well described in terms of those of $Cu_{2.33}V_4O_{11}$, $CuVO_3$ and $\beta$-$Cu_xV_2O_5$. Thus, it is probable that the samples prepared by Saito *et al.* were not pure, and the observed magnetic transition is not a genuine property of $Cu_{2.33}V_4O_{11}$.

A steep increase in the susceptibility below 20 K indicates the existence of localized electrons. A probable source for the latter is paramagnetic ions and/or a phase transition leading to electron localization.

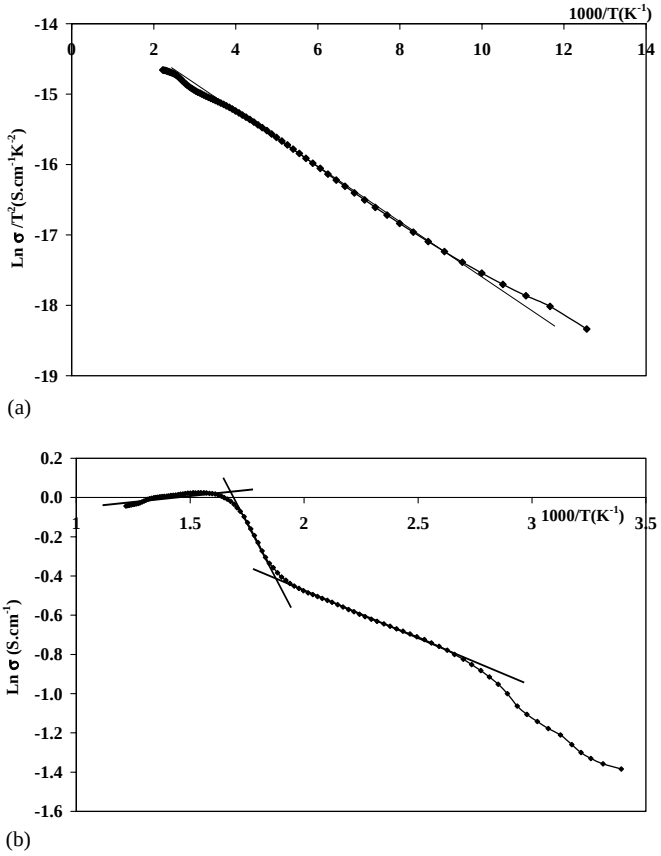


**FIG. 3.** Arrhenius plots of the electrical resistivity of $Cu_{2.33}V_4O_{11}$ in the (a) low- and (b) high-temperature regions.

## 5. X-RAY PHOTOELECTRON SPECTRA

Figure 5a shows the XPS spectra of pure Cu (dashed line) and $Cu_{2.33}V_4O_{11}$ (solid line). The binding energies (BE's) of the Cu $2p_{3/2}$ and $2p_{1/2}$ levels of pure Cu element are 932.4 and 952.3 eV, respectively, and the corresponding

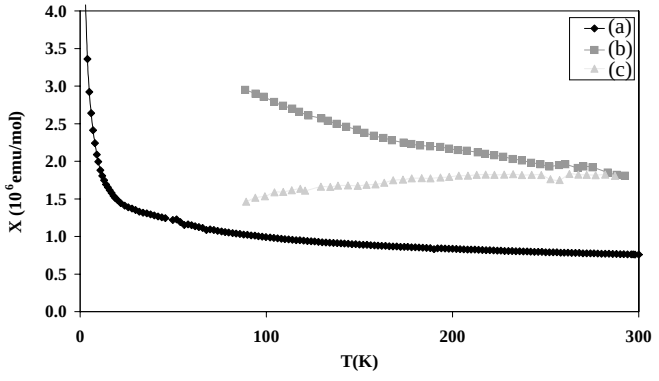


**FIG. 4.** Temperature dependence of the magnetic susceptibility of (a) $Cu_{2.33}V_4O_{11}$, (b) $CuVO_3$ and (c) $Cu_xV_2O_5$.

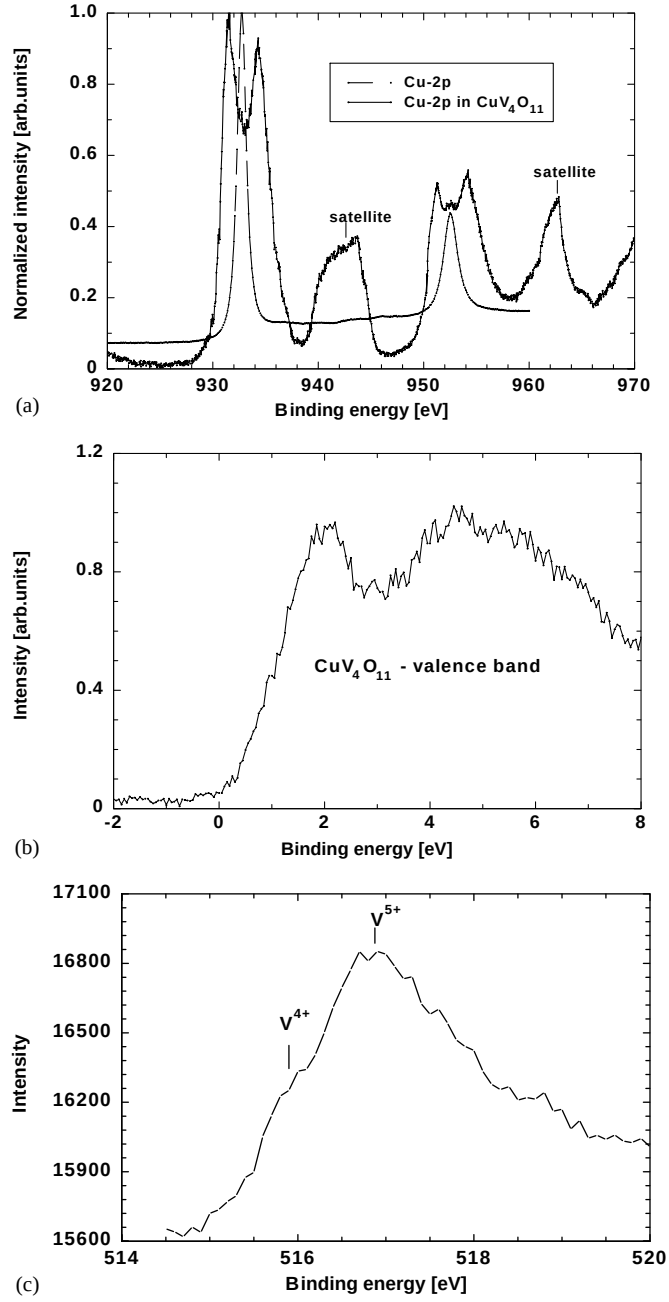


**FIG. 5.** XPS spectra of $Cu_{2.33}V_4O_{11}$: (a) Cu $2p_{3/2}$, (b) valence band and (c) V $2p_{3/2}$.

levels of $Cu_{2.33}V_4O_{11}$ are each split into two peaks. There occur high-intensity shake-up satellites at $\sim$10 eV higher than the main Cu $2p_{3/2}$ and $2p_{1/2}$ peaks. Such broad satellites are usually observed in compounds containing $Cu^{2+}$ ions. The Cu $2p_{3/2}$ peaks at 931.5 and 934.2 eV are assigned to $Cu^{+}$ and $Cu^{2+}$, respectively (15). Figure 5c shows the V $2p_{3/2}$ spectrum of $Cu_{2.33}V_4O_{11}$, which consists of two overlapping peaks. The peak at BE = 517 eV is

attributed to $V^{5+}$ ions, and the one at BE = 516 eV to $V^{4+}$ ions. The XPS valence band spectrum of $Cu_{2.33}V_4O_{11}$ is shown in Fig. 5b. The broad peak above 4 eV is assigned to the O 2*p*-block bands, and the main peak located near 2 eV to the occupied *d*-block bands of Cu and V (see Section 6).

The $[Cu^+]/[Cu^{2+}]$ ratio in $Cu_{2.33}V_4O_{11}$ can be estimated by integrating the areas of their Cu $2p_{3/2}$ peaks. According to Fig. 5a, this ratio is close to 1.11. Due to the overlap of the V $2p_{3/2}$ peaks of $V^{4+}$ and $V^{5+}$ ions (Fig. 5b), it is not possible to determine the $[V^{4+}]/[V^{5+}]$ ratio directly from the XPS spectrum. Given that $[Cu^+]/[Cu^{2+}] = 1.11$, the charge balance requirement shows that the $V^{4+}$ and $V^{5+}$ ions are present in $Cu_{2.33}V_4O_{11}$ in the ratio $[V^{4+}]/[V^{5+}] = 0.56$.

## 6. ELECTRONIC STRUCTURE CALCULATIONS

Let us examine the occurrence of mixed valence in Cu and V from the viewpoint of the average crystal structure of $Cu_{2.33}V_4O_{11}$ (9). As already mentioned, there are two types of Cu ion channels (Fig. 1b). Each first-type channel consists of two distorted $CuO_4$ tetrahedral sites per unit cell, while the second-type channel consists of two linear $CuO_2$ and two trigonal planar $CuO_3$ sites per unit cell. To avoid the occurrence of unreasonably short Cu–Cu distances along the channels, each $CuO_4$ tetrahedral site cannot be occupied by more than 50%. Likewise, each linear $CuO_2$ or trigonal planar $CuO_3$ site cannot be occupied by more than 33%. In general, linear $CuO_2$ and

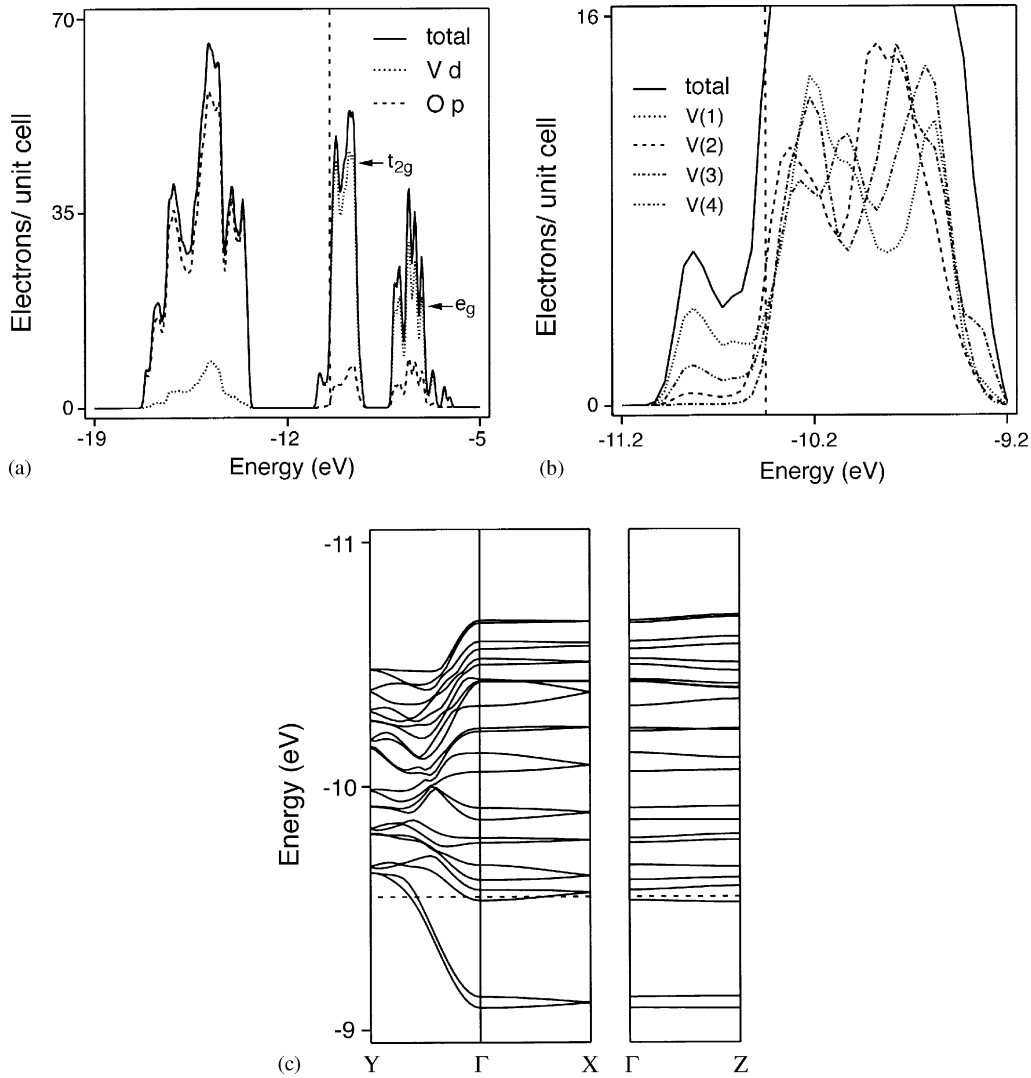


**FIG. 6.** (a) Total and partial densities of states curves. (b) Zoomed-in view of the bottom portion of the $t_{2g}$-block bands. (c) Dispersion relations of the $t_{2g}$-block bands, where $\Gamma = (0, 0, 0)$, $X = (a^*/2, 0, 0)$, $Y = (0, b^*/2, 0)$.

trigonal planar $CuO_3$ units occupied by $Cu^+$ ions. In addition, our electronic structure calculations for the $CuO_n$ ($n = 2, 3, 4$) units show that the highest-lying *d*-block level is higher in energy for the $CuO_4$ tetrahedral unit than for the linear $CuO_2$ and trigonal planar $CuO_3$ units (by 0.3 eV). Consequently, the oxidation state +2 should be assigned to the Cu ions of the first-type channels, and +1 to those of the second-type channels. This predicts that the $[Cu^+]/[Cu^{2+}]$ ratio is 1.33, so the $[V^{4+}]/[V^{5+}]$ ratio is 0.50, in $Cu_{2.33}V_4O_{11}$. These results are close to those deduced from the XPS study.

Since the Cu sites of $Cu_{2.33}V_4O_{11}$ are partially occupied, we perform electronic band structure calculations for the $(V_4O_{11})^{3.33-}$ lattice, i.e., the $V_4O_{11}$ lattice of $Cu_{2.33}V_4O_{11}$ in which the Cu ions in the first- and second-type channels are considered to donate two and one electron to the lattice, respectively. Figure 6a shows the density of states (DOS) calculated for the $(V_4O_{11})^{3.33-}$ lattice, where the solid line represents the total DOS, and the dotted line the partial DOS calculated for the V 3*d*-orbital contributions. Here, the Fermi level is shown for the normal metallic state in which there is no electron localization. There are 1.33 *d*-electrons per formula unit, i.e., 2.66 *d*-electrons per unit cell to fill the $t_{2g}$-block bands of Fig. 6a, so that the Fermi level lies near the bottom of the $t_{2g}$-block bands. The occupied region of the $t_{2g}$-block bands is about 0.5 eV wide. The top of the oxygen *p*-block bands lie about 3 eV below the Fermi level. According to our calculations for the $CuO_n$ ($n = 2, 3, 4$) clusters, the *d*-block levels of Cu in $Cu_{2.33}V_4O_{11}$ should lie in the region 2.7–3.5 eV below the Fermi level. This supports the assignment of the XPS valence band spectrum of $Cu_{2.33}V_4O_{11}$ given in the previous section.

A zoomed-in view of the DOS plots around the bottom part of the $t_{2g}$-block bands is presented in Fig. 6b, where the partial DOS plots for the 3*d*-orbital contributions from the four non-equivalent V atoms are shown. The 3*d*-orbital contributions to the occupied *d*-block bands come primarily from the V(1) and V(4) atoms, and the V(1) contribution is twice the V(4) contribution. Figure 1a shows that the $V_4O_{11}$ layer is made up of edge-sharing $V_4O_{12}$ ribbons, which are joined by corner sharing to form V(1)–O–V(4) bridges. The V(1) and V(4) atoms form the outer part of each $V_4O_{12}$ ribbon, and the V(2) and V(3) atoms the inner part of each $V_4O_{12}$ ribbon. Thus our calculations show that the $V^{4+}$ ions of $Cu_{2.33}V_4O_{11}$ are present in the outer part of each $V_4O_{12}$ ribbon, and the $V^{5+}$ ions in inner part of each $V_4O_{12}$ ribbon. The dispersion relations of the $t_{2g}$-block bands of the $(V_4O_{11})^{3.33-}$ lattice are presented in Fig. 6c, which shows the presence of three partially filled bands. The bottom two partially bands are dispersive primarily along the *b*-direction, and are almost separated out from the remaining $t_{2g}$-block bands that are narrow. This explains why the DOS of the $t_{2g}$-block bands is small below the Fermi level and becomes large above the Fermi level (Fig. 6a).

## 7. CONCLUDING REMARKS

The present magnetic susceptibility data of $Cu_{2.33}V_4O_{11}$ exhibit no evidence for a magnetic transition around 300 K and hence do not support the report by Saito *et al.* (7). The homogeneity range of $Cu_{2.33-x}V_4O_{11}$ is very narrow, and synthetic attempts to prepare this compound for *x* value outside the homogeneity range lead to a mixture of $Cu_{2.33}V_4O_{11}$, $CuVO_3$ and $\beta$-$Cu_xV_2O_5$. It is probable that the magnetic transition observed by Saito *et al.* is not based on a homogeneous sample of $Cu_{2.33}V_4O_{11}$. Our XPS spectra of $Cu_{2.33}V_4O_{11}$ reveal the presence of mixed valence in both Cu and V. The $[Cu^+]/[Cu^{2+}]$ ratio is estimated to be 1.11 from the Cu $2p_{3/2}$ peaks, and this leads to the ratio $[V^{4+}]/[V^{5+}] = 0.56$ by charge balance requirement. Our electronic structure calculations suggest that the oxidation state of the Cu ions is +2 in the channels of $CuO_4$ tetrahedra, and +1 in the channels of linear $CuO_2$ and trigonal planar $CuO_3$ units. This predicts that $[Cu^+]/[Cu^{2+}] = 1.33$ and $[V^{4+}]/[V^{5+}] = 0.50$ in $Cu_{2.33}V_4O_{11}$, which are consistent with those deduced from the XPS study. Our calculations show that the $V^{4+}$ ions of $Cu_{2.33}V_4O_{11}$ are present in the outer part of each $V_4O_{12}$ ribbon, and the $V^{5+}$ ions in the inner part of each $V_4O_{12}$ ribbon.

## ACKNOWLEDGMENTS

The work at North Carolina State University was supported by the Office of Basic Energy Sciences, Division of Materials Sciences, US Department of Energy, under Grant DE-FG05-86ER45259. The works at CEMES (France) and Institut of Physics (Poland) were supported by the CNRS, French and Polish governments via a Polonium program.

## REFERENCES

1. J. Galy, *J. Solid State Chem.* **100,** 209 (1992).
2. A. Casalot, Thèse Doctorat, Université de Bordeaux, 1968.
3. J. Galy, D. Lavaud, A. Casalot, and P. Hagenmuller, *J. Solid State Chem.* **2,** 531 (1970).
4. J. M. Savariault, E. Deramond, and J. Galy, *Z. Kristallogr.* **209,** 405 (1994).
5. J. Galy, J. Darriet, A. Casalot, and J. B. Goodenough, *J. Solid State Chem.* **1,** 339 (1970).
6. J. Galy, and D. Lavaud, *Acta Crystallogr. B* **27,** 1005 (1971).
7. Y. Sato, M. Onoda, and H. Nagasawa, *J. Phys. Soc. Jpn* **61,** 3865 (1992).
8. K. Kato, and K. Kasuda, *Z. Kristallogr.* **211,** 522 (1996).
9. P. Rozier, C. Satto, and J. Galy, *Solid State Sci.* **2,** 595 (2000).
10. R. L. Withers, and P. Rozier, *Z. Kristallogr.* **215,** 688 (2000).
11. P. Rozier, and S. Lidin, to be published.

12. M.-H. Whangbo, and R. Hoffmann, *J. Am. Chem. Soc.* **100,** 6093 (1978).
13. Our calculations were carried out by employing the *CAESAR* program package (J. Ren, W. Liang, M. -H. Whangbo, "Crystal and Electronic Structure Analysis Using CAESAR," 1998, http://www.PrimeC.com/.)
14. A. Casalot, D. Lavaud, J. Galy, and P. Hagenmuller, *J. Solid State Chem.* **2,** 544 (1970).
15. S. Poulston, P. M. Parett, P. Stone, and M. Bowker, *Surf. Interface Anal.* **24,** 811 (1996).
16. J. Ammeter, H.-B. Bürgi, J. Thibeault, and R. Hoffmann, *J. Am. Chem. Soc.* **100,** 3686 (1978).